Chemosphere 282 (2021) 131063

Contents lists available at ScienceDirect

Chemosphere

journal homepage: www.elsevier.com/locate/chemosphere

Copper transformation, speciation, and detoxification in anoxic and suboxic freshwater sediments

E.C. Cervi [a,*], S. Clark [b], K.E. Boye [c], J.P. Gustafsson [d], S. Baken [e], G.A. Burton Jr. [b]

[a] Golder Associates Brazil, Belo Horizonte, MG 30112-010, Brazil
[b] School for Environment and Sustainability, University of Michigan, Ann Arbor, MI 48109, USA
[c] Stanford Synchrotron Radiation Lightsource, SLAC National Laboratory, Menlo Park, CA 94025, USA
[d] Department of Soil and Environment, Swedish University of Agricultural Sciences, 750 07 Uppsala, Sweden
[e] European Copper Institute, Brussels, B-1150, Belgium

ARTICLE INFO

Handling Editor: Milena Horvat

Keywords:
Geochemical speciation
Copper
EXAFS/XANES
Raman spectroscopy
Hyalella azteca
Daphnia magna
Aquatic toxicity

ABSTRACT

The complex chemistry of copper (Cu) in freshwater sediments at low concentrations is not well understood. We evaluated the transformation processes of Cu added to freshwater sediments under suboxic and anoxic conditions. Freshwater sediments from three sources in Michigan with different characteristics (Spring Creek, River Raisin, and Maple Lake) were spiked with 30 or 60 mg kg^{-1} Cu and incubated under a nitrogen atmosphere. After 28-d, each treatment subset was amended with organic matter (OM) to promote anoxic conditions and evaluate its effects on Cu speciation. OM addition triggered a shift from suboxic to anoxic conditions, and sequential extractions showed that Cu accordingly shifted from acid-soluble to oxidizable fractions. Extended X-ray absorption fine-structure (EXAFS) spectroscopy revealed that Cu sulfides dominated all anoxic samples except for Spring Creek 30 mg kg^{-1}, where Cu(I) was predominantly complexed to thiol groups of OM. Covellite and chalcopyrite ($CuFeS_2$) were the predominant Cu species in nearly all anoxic samples, as determined by Raman spectroscopy, scanning electron microscopy, and X-ray absorption near-edge structure (XANES) spectroscopy. Copper reduction also occurred under suboxic conditions: for two of three sediments, around 80% had been reduced to Cu(I), while the remaining 20% persisted as Cu(II) complexed to OM. However, in the third coarsest (i.e., Spring Creek), around 50% of the Cu had been reduced, forming Cu(I)-OM complexes, while the remainder was Cu(II)-OM complexes. Toxicity tests showed that survival of *H. azteca* and *D. magna* were significantly lower in suboxic treatments. Anoxic sediments triggered a near-complete transformation of Cu to sulfide minerals, reducing its toxicity.

1. Introduction

Metal contamination in aquatic environments is a significant issue (Luoma and Rainbow, 2008; Jeppe et al., 2017, Burton Jr. et al., 2019). Copper (Cu) is particularly problematic due to its toxicity and prevalence in aquatic sediments from various sources, including stormwater runoff, sewer discharge, fossil fuel combustion, mining effluent, and other industrial waste (Khangarot and Das, 2010; Fukunaga and Anderson, 2011). Our limited understanding of the bioavailability of Cu in sediments has hampered our ability to protect biota in aquatic environments from the harmful effects of Cu contamination in sediments (Besser et al., 2003).

We do know that Cu distribution is affected by the pH and oxidation-reduction potential of aquatic environments and the presence of any competing metal ions or inorganic anions (Simpson, 2005; Rader et al., 2019). Sulfate reduction and vertical redox zonation in sediments are also affected by environmental conditions, including the amounts of dissolved oxygen (DO), the amounts and reactivity of organic carbon (OC), the availability of sulfate and other electron acceptors (such as nitrate, Mn(IV), and Fe(III)), sedimentation rates, and grain size (Jørgensen and Kasten, 2005). The fate of Cu is affected by its ability to bind to many types of dissolved ligands and solid phases, which means it transforms and fluxes in the aquatic environment in various compartments (Di Toro et al., 2001a; Cantwell et al., 2008).

After introducing Cu into sulfate-reducing anoxic sediment, an obvious candidate for Cu immobilization is sulfide (Simpson et al.,

* Corresponding author.
E-mail address: ecervi@golder.com (E.C. Cervi).

https://doi.org/10.1016/j.chemosphere.2021.131063
Received 13 April 2021; Received in revised form 19 May 2021; Accepted 28 May 2021
Available online 3 June 2021

2012). For this reason, the popular method to evaluate environmental risk in this environment is to determine the concentration of acid volatile sulfide (AVS) and simultaneously extracted metals (SEM) (Burton et al., 2007). It is widely recognized that the porewater concentrations of SEM will be negligible when sediments contain a molar excess of AVS over SEM, and that acute or chronic toxicity should not result from metals in these conditions (USEPA, 2005; Simpson et al., 2012). However, this methodology does not consider differences in sediment properties that impact Cu bioavailability (Campana et al., 2012) and relies on a picture of the Cu chemistry that is vastly oversimplified (Weber et al., 2009; Zhang et al., 2014).

The Cu–S system is complex and contains many dissolved, colloidal, and crystalline phases.

According to Gardham et al. (2014) for sediments with Cu concentrations >65 mg kg^{-1} [Interim Sediment Quality Guidelines-Low of the ANZECC/ARMCANZ (2000) guidelines], partition coefficients (K_d) generally range from 1×10^4 to 1×10^6 L kg^{-1} (between the sediment and pore water) and from 1×10^3 to 2×10^5 L kg^{-1} (between the sediment and overlying water). As indicated by these K_d, naturally contaminated environments generally have low concentrations of dissolved Cu. Because dissolved metals are usually more bioavailable than solid-phase particles, this partitioning is an important factor that influences bioavailability and bioaccumulation in aquatic biota (Ahlf et al., 2009; Fukunaga and Anderson, 2011).

Copper is an active redox element, and it can be reduced – by abiotic or biotic processes – from cupric Cu(II) to cupreous Cu(I) or Cu(0) (Fulda et al., 2013a). The reduction of Cu(II) in sulfate-reducing conditions by dissolved sulfide (Luther et al., 2002) and the resultant precipitation of sparingly-soluble metal sulfides (Morse and Luther, 1999) may substantially decrease the solubility of Cu. In the presence of S(-II), Cu(II) is reduced to Cu(I) and then precipitated with S(-I) to form amorphous covellite, CuS(s) (Patrick et al., 1997). However, during the flooding of initially oxic sediment, Cu(II) was found to be reduced to Cu(I) first and then reduced to Cu(0) before the start of sulfate reduction. When this eventually occurred, Cu was slowly transformed to Cu(I)-sulfide precipitates (Weber et al., 2009). Moreover, Cu(II) may be reduced to Cu(I) by organic substances (Pham et al., 2012; Fulda et al., 2013b) and the formed Cu(I) may also form strong complexes with organic matter (OM) (Karlsson et al., 2006; Fulda et al., 2013a). Particularly in sediments where the content of available sulfide is low, organic Cu(I) and Cu(II) complexes may constitute a considerable fraction of the geochemically active Cu (Fulda et al., 2013b).

Previous studies on the mobilization of Cu during anoxic to suboxic transitions were primarily focused on the oxidative dissolution of Cu sulfides in sulfide-rich sediments (e.g., Caetano et al., 2003; Fulda et al., 2013a). In order to predict Cu toxicity, it is therefore critical to understand Cu speciation and bioavailability under many conditions. The aim of this study is to investigate the mechanisms that transform dissolved Cu in oxic overlying/porewater to non-bioavailable solid-phase species during the transition to suboxic and anoxic conditions.

2. Materials and methods

2.1. Sediment collection and characterization

A shovel was used to collect surficial sediments (at 0–10 cm depths) from three freshwater ecosystems in Michigan (USA): River Raisin and Spring Creek, which are low-gradient streams, and Maple Lake, which is a small reservoir on the Paw Paw River (south branch). These sites have no history of metal contamination and were selected because they differed in key metal-binding ligands, such as SEM, AVS (Burton et al., 2007), total iron (Fe), and OM (Table 1).

Most significantly, Raisin sediments had OM contents (loss-on-ignition – LOI = 5.9%) that was about 6 and 19-fold greater than those in Spring Creek and Maple Lake, respectively (Table 1). Low AVS concentrations (<1.2 μmol g^{-1}) suggest a limited contribution of sulfide phases to metal binding in the sediments from all three locations, especially for Spring Creek. The OC normalized difference between SEM and AVS [SEM-AVS/(f_{OC})] ranged from −228.8 to 14.2 μmol g^{-1} OC. Metal toxicity is predicted when SEM-AVS/(f_{OC}) > 150 μmol g^{-1} OC. Raisin sediments, relative to Spring and Maple sediments, had greater amounts of total organic carbon (TOC = 3.3%, 0.4% and 0.3%, respectively) and Fe (7,560, 2640 and 2370 mg kg^{-1}, respectively).

Table 1
Physicochemical properties of studied sediments collected from River Raisin, Spring Creek, and Maple Lake.

Variable	River Raisin	Spring Creek	Maple Lake
pH	6.3	6.1	6.4
Organic matter (loss on ignition, %)	5.9	0.9	0.3
Total organic carbon (TOC, %)	3.3	0.4	0.4
Total Fe (mg kg^{-1} dw)	7563	2644	2367
Total Mn (mg kg^{-1} dw)	506	71.0	41.0
Total Cu (mg kg^{-1} dw)	BDL[a]	6.8	1.0
AVS (μmol g^{-1})	1.12	<0.05	1.18
SEM-AVS/(f_{OC}) (μmol g^{-1})	14.2	7.6	−228.8
Coarse (%)	5.1	31.9	1.2
Medium (%)	90.8	48.0	97.7
Fines (%)	2.7	16.0	1.0

[a] Below detection limit (= 0.26 mg $kg^{-1}$for Cu).

Sediment temperature, dissolved oxygen (DO), and pH were measured immediately after on-site sampling and throughout the laboratory incubation period. Temperature was measured using a digital thermometer and DO and pH were measured using microsensors and a four-channel Microsensor Multimeter (Unisense® A/S, Denmark). SensorTrace PRO® software (Unisense® A/S, Denmark) was used for sensor signal logging. Two points were used to calibrate the DO sensor: air saturated tank water (100% air saturation) and an anoxic solution of 2 g sodium ascorbate in 100 mL of 0.1 M NaOH (0% saturation). The detection limit for DO was 0.05 μM. The pH sensor calibration was done in buffers with pH of 4.0, 7.0, and 10.0.

2.2. Experimental setup

Fig. 1 shows the experimental setup to investigate the transformation processes of Cu added to freshwater sediments under suboxic and anoxic conditions. Briefly, a 28-d laboratory incubation of the sediments was performed with spiked Cu (30 and 60 mg kg^{-1} Cu) under a nitrogen atmosphere. Sediments at background concentrations (without spiking) were used as control. After 28-d, a subset of each treatment was amended with OM and sediments were incubated for another 28-d to evaluate the effects of anoxic conditions on Cu speciation. Sediment physicochemical characterization included total metals, TOC, SEM/AVS, and particle size. A BCR-701 protocol quantified geochemical fractions of Cu. In addition, the speciation of S and Cu was determined using X-ray absorption near edge structure (XANES) and extended X-ray absorption fine structure (EXAFS) spectroscopy, respectively. Scanning electron microscopy and energy dispersive system (SEM/EDS) analysis and Raman spectroscopy were performed for microstructural and mineralogical characterization. Toxicity tests evaluated the effects of Cu in overlying water and surficial sediments using *Daphnia magna* and *Hyalella azteca*, respectively.

2.3. Preparation of Cu-spiked sediments

Sediments were spiked with Cu using an indirect procedure and pH adjustment (Simpson et al., 2004; Costello et al., 2015). All experiments were done in triplicate within an anaerobic chamber (Coy, 95% N_2/5% H_2) using N_2-purged solutions, which were prepared using ultrapure deionized water (Millipore, 18.2 MΩ cm) and analytical grade chemicals. A small volume (approximately 1 L) of sediment was modified with copper chloride dihydrate ($CuCl_2{\cdot}2H_2O$, Sigma Aldrich), sealed under

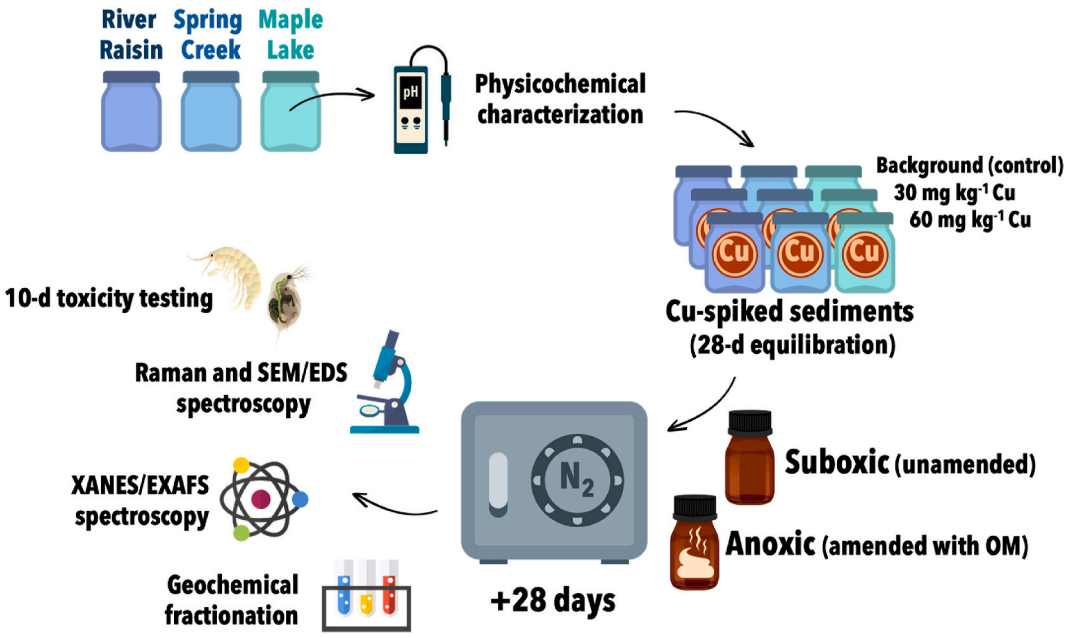

Fig. 1. Schematic of the stepwise process for the copper transformation experiments.

N_2 headspace, and then shaken to mix for 1 h. After 24 h, a small amount of 1 M NaOH was added to modify sediment pH to be near the initial pH, within 0.5 units. After 7 days, spiked sediments were diluted using reference sediments to create Cu target concentrations. Nominal metal concentrations were selected to span an expected nontoxic (30 mg kg^{-1} Cu) to possibly toxic (60 mg kg^{-1} Cu) range to *Hyalella azteca* and *Daphnia magna* (Roman et al., 2007). Sediments at background concentrations (without spiking) were used as the control. Spiked sediments were incubated for 28 days under N_2 (rolled 2 h, three times per week) to allow sufficient time for Cu equilibration to be reached between pore water and solid-phase fractions.

2.4. Organic matter amendments

After 28 days of incubation, we evaluated the transformation processes of Cu added to freshwater sediments under what is generally defined (e.g., Tostevin and Poulton, 2019) as suboxic (DO of 1–10 μM) and anoxic (DO < 1 μM) conditions. To achieve this, the Cu-spiked sediments were either unamended (suboxic) or amended (anoxic) with OM from animal feces. For the OM-amendment, an aliquot of approximately 50 g (dry weight) OM was added to 10 mL of MilliQ water and homogenized to create a slurry (initial TOC = 3.8%). To avoid excessive bacterial activity and maintain environmentally realistic conditions, the slurry was mixed in 1 L of formulated sediment (slurry/sediment ratio 1:20) and rolled for 24 h to create a target concentration of ~1% TOC. Both unamended and OM-amended sediments were incubated inside an anaerobic chamber for another 28 days before analysis.

Total OC was determined for all sediments at all treatment conditions. Sediment samples (~10 g wet weight) were shipped to the Alfred H. Stockard Lakeside Laboratory at the University of Michigan Biological Station for analysis. Upon arrival, all sediments were homogenized and freeze-dried at approximately −80 °C and subsequently analyzed in the elemental analyzer (OI Analytical, model 1080), in accordance with U.S. EPA method 440.0 (Zimmerman et al., 1997).

2.5. Copper fractionation in suboxic and anoxic sediments

The suboxic and anoxic sediment samples were sequentially extracted to determine four geochemical fractions of Cu using the modified three-stage BCR procedure (Davutluoglu et al., 2011), which has good reproducibility and recoveries. This procedure is described in detail in Table 2, which also contains the target phases each extraction is assumed to represent. However, the accuracy of this assignment has often been debated. For example, Donner et al. (2012) observed that organically complexed Cu to a large extent is extracted into the reducible (F2) fraction, which is explained by the low pH (1.5) of the extract. Hence in our analysis we interpret the results primarily in terms of changes in the relative solubility of Cu, rather than to assign the extracted Cu to specific phases. The extraction was done using ~1 g of wet sediment at different nominal concentrations (background, 30 mg kg^{-1} Cu, and 60 mg kg^{-1} Cu) in 50 mL polypropylene centrifuge tubes. After each extraction, mixtures were centrifuged at 3000 rpm for 20 min. The supernatant was then decanted and stored in clean centrifuge tubes at 4 °C until analysis.

The sediment residue from each extraction was then washed using

Table 2
The modified BCR three-stage extraction procedure.

Step (Fraction)	Nominal target phase(s)	Reagent(s)	Procedure(s)
F1 (Exchangeable, water and acid soluble)	Soluble species, carbonates, exchangeable metals	0.11 mol L^{-1} CH_3COOH	20 mL CH_3COOH + 0.5 g sample shaken 30 rpm-16 h
F2 (Reducible)	Iron/manganese oxyhydroxides	0.5 mol L^{-1}, $NH_2OH{\cdot}HCl$ (adjusted to pH 1.5 with HNO_3)	20 mL $NH_2OH{\cdot}HCl$ + residue from step 1 and shaken 30 rpm-16 h
F3 (Oxidizable)	Organic matter and sulfides	8.8 mol L^{-1} H_2O_2 followed by 1.0 mol L^{-1} CH_3COONH_4 (adjusted to pH 2 with HNO_3)	10 mL H_2O_2 + residue from step 2 at 85 °C till almost dryness; 25 mL CH_3COONH_4 shaken 30 rpm-16 h
Residual[a]	Remaining, non-silicate bound metals	Nitric acid digestion	Costello et al. (2019)

[a] Digestion of residual material is not included in the original BCR protocol (Davutluoglu et al., 2011).

10 mL Milli-Q water and shaken mechanically for 15 min at 30 rpm. Following shaking, residue was centrifuged at 3000 rpm for 20 min. The supernatant was discarded. The results of the sequential extraction procedure were verified by comparing the sum of the four steps (acid soluble + reducible + oxidizable + residual) with the total Cu content, which was determined by digesting dried sediment with concentrated nitric acid (HNO_3) in a hot block at reflux temperatures (Environmental Express) (Costello et al., 2019). Metal concentrations were determined using inductively coupled plasma-optical emission spectroscopy (ICP-OES, Perkin Elmer, model Optima 8000) and the USEPA method 6010B for Cu (USEPA, 1996).

The percentage recovery from the digestion was verified (>80%) by using the Commission of the European Communities Bureau of Reference (BCR) BCR-701 certified reference material in the digestion. Recoveries of acid soluble, reducible, oxidizable, and residual fractions for the BCR-701 reference material were 98%, 114%, 84%, and 103%, respectively (Supplemental Data, Figure S1), compared to the values certified by the European Commission (Rauret et al., 2001). A satisfactory recovery of 95% was obtained for the total digestion of the certified reference material BCR-701.

2.6. Raman and SEM/EDS spectroscopy

The morphology, speciation and chemical composition of the sediments were analyzed on suboxic and anoxic wet samples (spiked with 60 mg kg^{-1} Cu) using a TESCAN Mira 3 GMU (TESCAN, Brno, Czech Republic). The Mira 3 scanning electron microscope was coupled to an EDAX Team (EDAX, Mahwah, USA) energy dispersive system (SEM/EDS) with elemental mapping capabilities as well as with a confocal Raman microscope for comprehensive correlative sample analysis. The SEM/EDS imaging adopted the following analytical conditions: an acceleration voltage of 5 kV, a beam intensity of 8 nA and a magnification of 5kX, 10kX, and 20kX. The EDS operating conditions involved an accelerating voltage of 20 kV and a resolution of 123.8 eV.

The SEM/EDS stage was used for transferring a sample to the Raman imaging position (automated movement). The advantage of this coupled system is its ability to conduct different analyses for the same regions of interest. In this study, 2-dimensional Raman spectral maps (X, Y) were collected and then analyzed to determine the mineralogical composition of the sediments. The areas of interest were identified using SEM/EDS imaging and microanalysis. The excitation wavelength was 785 nm, with a power of 30 mW. The Raman spectra were recorded from −580 to 3000 cm^{-1} (accumulation time of 0.5 s).

2.7. X-ray absorption near-edge structure (XANES)

X-ray absorption spectroscopy (XAS) was used to determine S, Fe, and Cu speciation in the suboxic and anoxic sediments. XAS measurements were performed at the beamlines 4-3 (S K-edge) and 7-3 (Cu and Fe K-edges) of the Stanford Synchrotron Radiation Lightsource (SSRL, SLAC National Accelerator Laboratory, Menlo Park, USA). Freeze-dried (liquid N_2) samples were placed on S-free XRF Mylar tape (Fluxana GmbH & co. KG, Bedburg-Hau, Germany) across a 2 × 4 cm^2 window in an aluminum frame. Samples were covered with a 5 μm thick polypropylene film and kept under a positive helium flow during measurements (Almkvist et al., 2010; Boye et al., 2011).

S K-edge XANES data were collected across an energy range from 2422 to 2618 eV in fluorescence mode using a 7-element Ge array detector. The beamline was equipped with a Si[111] double-crystal monochromator. To reduce higher-order harmonics, the monochromator was detuned 30% of maximum intensity during the measurements. To minimize beam damage and thermal disorder, all samples were measured in a He cryostream operating at 15 K. Internal energy calibration was performed using the white line energy of a sodium thiosulfate standard, which was assigned to 2472.02 eV (Boye et al., 2011). Calibration was conducted at the beginning of the analysis and then after every five sample scans. Three or four scans were collected per sample.

Each raw S XANES spectrum was individually analyzed to remove poor scans before merging, alignment and normalization using the software Demeter Athena XAS Data Processing, version 0.9.26 (Ravel and Newville, 2005), following the procedures described by Kelly et al. (2008). The samples were normalized using a pre-edge range for baseline adjustment of −25 to −7 eV relative to E_0, and a post-edge normalization range from +50 to +70 eV relative to E_0, keeping the E_0 constant at 2472.02 eV. The S K-edge XANES spectra were interpreted qualitatively using spectra from standard compounds (Table 3), diluted 1:6 with boron nitride to minimize self-absorption, which had been previously recorded at the same beamline (Boye et al., 2011). The standards were grouped into S forms: reduced (peak energy <2475 eV), intermediate (peak energy 2475–2479 eV) and highly oxidized (peak energy>2479 eV).

For the Cu K-edge, XANES data were collected in fluorescence mode using a 30-element Ge array detector. The beamline was equipped with a Si[220] double crystal monochromator and a He cryostat (<15 K). The Fe fluorescence and scattering contributions were reduced using a combination of Ni and Al filters together with Soller slits. Internal energy calibration was accomplished using a metallic copper foil assigned to 8979 eV (Thompson et al., 2009). Multiple scans, from 3 to 8, were done on each sample. No systematic changes were observed in individual scans of the same samples, hence there was no evidence of beam damage.

Cu K-edge data were collected from −150 to −30 eV, and from +80 to +740 eV, respectively, relative to E_0, which was kept at 8988 eV. The Cu K-edge XANES spectra were compared to a collection of standards obtained from various sources, detailed in Table S1 (Supplemental Data). Linear combination fitting (Fulda et al., 2013b) was done to fit the sample spectra using weighted combinations of the standard spectra (Figure S2, Supplemental Data). In the fitting, no energy shifts were permitted. The fitting range was constrained to between −10 and +30 eV relative to E_0. At most three standards were included in each fit.

Fe K-edge XANES data were also collected at beamline 7-3. However, these data showed that for all samples the first shell was dominated by a mixture of Fe(II)–O and Fe(III)–O paths typical of primary minerals, and that phases of relevance for the current study, e.g. Fe–S minerals, could not be identified; therefore, these results were disregarded.

2.8. Extended X-ray absorption fine structure (EXAFS)

For Cu K-edge EXAFS, background removal was done using the AUTOBAK algorithm in Athena, with a *k*-weight of 3 and with the Rbkg parameter set to 0.9. The scans were then imported to Artemis (Ravel and Newville, 2005) for final treatment of the EXAFS spectra, producing a model for the first-shell contributions. For each sample, two models were tested, alone or in combination. In the first, Cu(I) was bound to 3 S at ~2.3 Å, similar to the coordination in covellite (Evans and Konnert,

Table 3
Sulfur standard compounds and functional groups included in the fitting of XAS sample spectra.

	Function	Sulfur Compound	Oxidation State	Maximum Peak (eV)
Reduced S	Sulfide	Iron sulfide	−2	2470.2
	Sulfhydryl	Elemental S	0	2472.5
		Cysteine	0	2473.5
Intermediate forms of oxidized S	Thiosulfate	Sodium dithiosulfate pentahydrate ($Na_2S_2O_3{\cdot}5H_2O$)	+2	2479.3
Highly oxidized S	Sulfonate	L-Cysteic acid	+5	2481.2
	Sulfate	Sodium sulfate decahydrate ($Na_2SO_4{\cdot}10H_2O$)	+6	2482.4

1976), and in the second Cu(II) was bound to 4 equatorial O in a Jahn-Teller coordination similar to that found in Cu(II) sorption complexes as in ferrihydrite (Tiberg et al., 2013).

During the fitting procedure, the amplitude reduction factor (S_0^2) was set to 0.98 (Fulda et al., 2013b), while the coordination numbers (CN) and the Debye Waller factors were allowed to vary. Because the CN:S and the Debye-Waller factors are interrelated, the optimised values for CN should not be given much weight in the interpretation. The *k*-range used was from 2.5 to 10 $Å^{-1}$, and the R+ΔR range was from 1 to 2.2 Å (corresponding to interatomic distances of 1.5–2.7 Å). EXAFS shell fitting was not performed for the Raisin River 30 mg kg^{-1} and Maple Lake 30 mg kg^{-1}, as these data were restricted to the XANES region.

2.9. Acute and chronic effects of copper to benthic invertebrates

Laboratory 10-day acute and chronic toxicity tests were completed in order to assess the effects of suboxic and anoxic Cu-spiked sediments. Tests were conducted using pelagic (*D. magna*, 3–4 days old) and epibenthic (*H. azteca*, aged 7–14 days) invertebrates exposed to overlying water and sediment + porewater, respectively. Test chambers were 300-mL beakers containing 100 mL of sediment and 175 mL of ion-enriched water (IEW). Ten individuals of each species were used in each of the four replicates. Test endpoints included survival and growth for *H. azteca* (USEPA, 2000), and survival, growth, and reproduction for *D. magna* (USEPA, 2002). *D. magna* were fed Sel-Cero every day during the exposure, while *H. azteca* were not fed to promote sediment grazing.

Three representative groups (10 organisms each) were collected to estimate initial mass on day 0 (±0.001 mg). Individual growth rate (IGR) for both organisms was calculated per Cervi et al. (2020) as follows:

$$\mathrm{IGR} = \frac{\left[\frac{\Sigma\left(\mathrm{mass_{org}}\right)_{\mathrm{final}}}{n_{\mathrm{org}}} - \frac{\Sigma\left(\mathrm{mass_{org}}\right)_{\mathrm{initial}}}{n_{\mathrm{org}}}\right]}{\mathrm{time}}$$

where mass is in μg, *n* is the number of organisms/replicates, and time is days.

2.10. Statistical analysis

Significant differences in Cu toxicity under suboxic and anoxic conditions were determined among the different Cu-spiked sediments and the control at background concentrations ($p < 0.05$). XLSTAT® statistical software for Microsoft® Excel was used and the following tests conducted: (1) Shapiro-Wilk to determine if datasets had normal or non-normal distributions, (2) Levene's test to determine whether variances among treatments were equal, (3) Kruskal-Wallis for multivariate comparisons of non-parametric variables, and (4) one-way analysis of variance (ANOVA) for multivariate comparisons of normally distributed variables, followed by Tukey's Honest Significant Difference post-hoc test as needed.

3. Results

3.1. Organic matter amendments

After 24h and throughout the 28-day incubation period, sediments amended with OM were anoxic (DO concentration = 0.0 mg L^{-1}), and unamended sediments were suboxic (DO concentration between 0.01 and 0.20 mg L^{-1}) (Figures S3A and S3B, Supplemental Data). For suboxic samples (unamended), %TOC ranged from 0.3 to 3.3% (mean of 1.1%), while for anoxic samples (OM-amended), the values ranged from 0.4 to 4.0% (mean of 1.4%). All sediments increased %TOC after OM amendments, except for River Raisin at 60 mg kg^{-1} Cu, which decreased from 2.0% (suboxic) to 1.8% after OM-amendments (Supplemental Data, Figure S4). Lower levels of %TOC were observed in samples at higher Cu concentrations, suggesting the presence of added Cu in the microcosms elicited OM consumption by stressed microorganisms (Dupont et al., 2011).

Over the 28-day experiment, the pH remained stable (pH 6.3 ± 0.0) in all suboxic sediments (Figure S3C, Supplemental Data). The pH at the start of the incubation was higher in anoxic than suboxic sediments, particularly for Raisin River and Spring Creek at background concentrations (both pH 6.8). The pH of anoxic sediments on day −1 of the experiment ranged between approximately 6.1 and 6.8 (Figure S3D, Supplemental Data). Following 24-h equilibration, there was an initial increase in pH in all anoxic samples, with pH on day 1 ranging between approximately 6.6 and 7.1. The pH then gradually increased from day 4–7 and plateaued after two weeks (day 14–28). Mean pH values in the anoxic sediments over the course of the experiment were: River Raisin = 6.8 ± 0.3, Spring Creek = 7.0 ± 0.3, and Maple Lake = 6.8 ± 0.3.

Temperatures across both unamended and OM-amended treatments (Figures S3E and S3F, Supplemental Data) were held rather constant over the study period (17.5–17.9 °C). The redox potential of all suboxic sediments (Figure S3G, Supplemental Data) remained rather constant over the study period (mean of 290 ± 10 mV). In contrast, the redox potential declined rapidly in anoxic sediments (Figure S3H, Supplemental Data) from day −1 to day 0 and remained stable after two weeks (day 14–28). This suggests that the added OM was decomposed, with subsequent consumption of oxygen, consumption of other terminal electron acceptors (e.g., nitrate), and decrease in redox potential.

3.2. Copper fractionation in suboxic and anoxic sediments

Measured concentrations of Cu-spiked sediments (Table 4) remained within 82–105% of the targeted range (30 or 60 mg kg^{-1}). Therefore, nominal concentrations were adopted throughout the study to improve readability. Copper was not detected in River Raisin sediments at background concentrations, whereas Cu in Spring Creek sediments under suboxic and anoxic conditions were 5.7 and 5.6 mg kg^{-1}, respectively.

Fig. 2 and Table S2 (Supplemental Data) shows the Cu geochemical fractionation in suboxic and anoxic sediments following the modified BCR-701 extraction procedure. Copper was almost entirely bound to extractable fractions (F1, F2 and F3) in all sediments. River Raisin sediments spiked with Cu (30 and 60 mg kg^{-1}) were mainly associated to the oxidizable fraction. The percentage of Cu bound to OM and sulfides were 82% and 91% (suboxic and anoxic samples, respectively) in River Raisin sediments spiked with 30 mg kg^{-1}, whereas 77% and 93% were bound to the same fraction in suboxic and anoxic sediments spiked with 60 mg kg^{-1}.

For suboxic Spring Creek sediments at background concentrations, Cu was heterogeneously bound to acid soluble (F1 = 5%), reducible (F2 = 38%), and oxidizable (F3 = 57%) fractions. Copper was mainly associated with the reducible fraction in both Cu-spiked suboxic sediments (55% and 67% for 30 and 60 mg kg^{-1}, respectively). Results for the Maple Lake sediments were similar. In the presence of OM,

Table 4
Nominal versus mean measured concentrations of River Raisin, Maple Lake, and Spring Creek sediments at background and Cu-spiked concentrations (30 and 60 mg kg^{-1}) under suboxic and anoxic conditions. Percentage of nominal concentration is given in parentheses.

Nominal concentration	River Raisin	Maple Lake	Spring Creek
	Measured concentration (mg kg^{-1})		
Background Suboxic	0.0	1.5	5.7
Background Anoxic	0.0	1.0	5.6
30 mg kg^{-1} Cu Suboxic	30.3 (101)	28.8 (96.1)	27.0 (90)
30 mg kg^{-1} Cu Anoxic	28.0 (93.3)	24.7 (82.3)	31.6 (105)
60 mg kg^{-1} Cu Suboxic	57.6 (96)	53.1 (88.4)	52.5 (87.4)
60 mg kg^{-1} Cu Anoxic	53.9 (89.8)	59.3 (98.8)	55.2 (92)

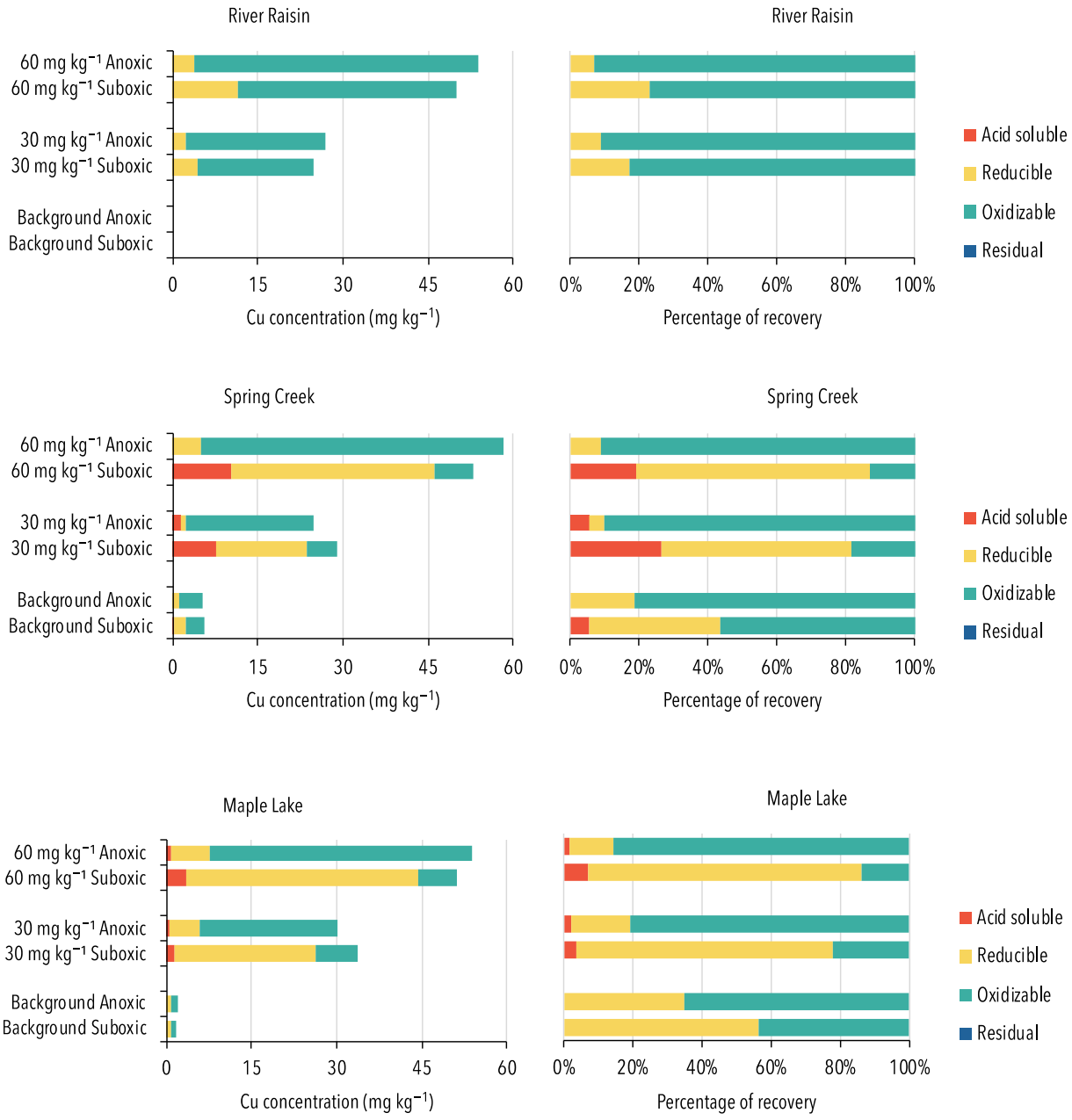

Fig. 2. Geochemical fractionation of copper (mg kg^{-1}) for suboxic and anoxic Maple Lake, Raisin River, and Spring Creek sediments at different spiked concentrations and analysis recovery using the BCR-701 extraction procedure and certified reference material.

oxidizable Cu became the dominant fraction for both sediments. For example, for Spring Creek F3 represented 90% and 91% of Cu for the anoxic sediments at 30 and 60 mg kg^{-1} spiked Cu, respectively. Collectively, these results show that the amendment of OM led to poorer Cu extractability, possibly because of Cu-sulfide formation.

3.3. Characterization of S species

The S K-edge XANES results were different for the sediments that were amended with OM compared to those that were not: the suboxic samples had a predominance of oxidized S species, particularly sulfate, whereas the content of reduced S, such as S(-I) and S(-II) was rather low (Fig. 3). In the anoxic samples, most of the sulfate had been reduced, increasing the fraction of reduced S species considerably. Hence, the anoxic samples had a larger concentration of both inorganic sulfide and organic sulfide/thiol compounds, with which spiked Cu could react.

Based on edge-normalized S K-edge XANES spectra of the reference compounds, six predominant S species were isolated across the experimental sediment samples: inorganic sulfides (represented by FeS), elemental S, cysteine, sodium dithiosulfate pentahydrate ($Na_2S_2O_3{\cdot}5H_2O$), L-cysteic acid, and sodium sulfate decahydrate ($Na_2SO_4{\cdot}10H_2O$). When categorized based on functional group and oxidation state, it was apparent that highly oxidized sulfates and sulfonates comprised the predominant species for all spectra, across all treatments, although the addition of OM influenced species concentrations.

Among anoxic sediments, we found a significant presence of inorganic sulfides and thiols, at peaks of 2470.2 and 2473.6 eV, respectively. Elemental S (2472.5 eV) was only observed in Maple Lake 30 mg kg^{-1} and 60 mg kg^{-1}. Decreased quantities of inorganic sulfides and sulfhydryl groups were detectable in suboxic sediments, suggesting that a higher fraction of the S species was present in oxidized forms.

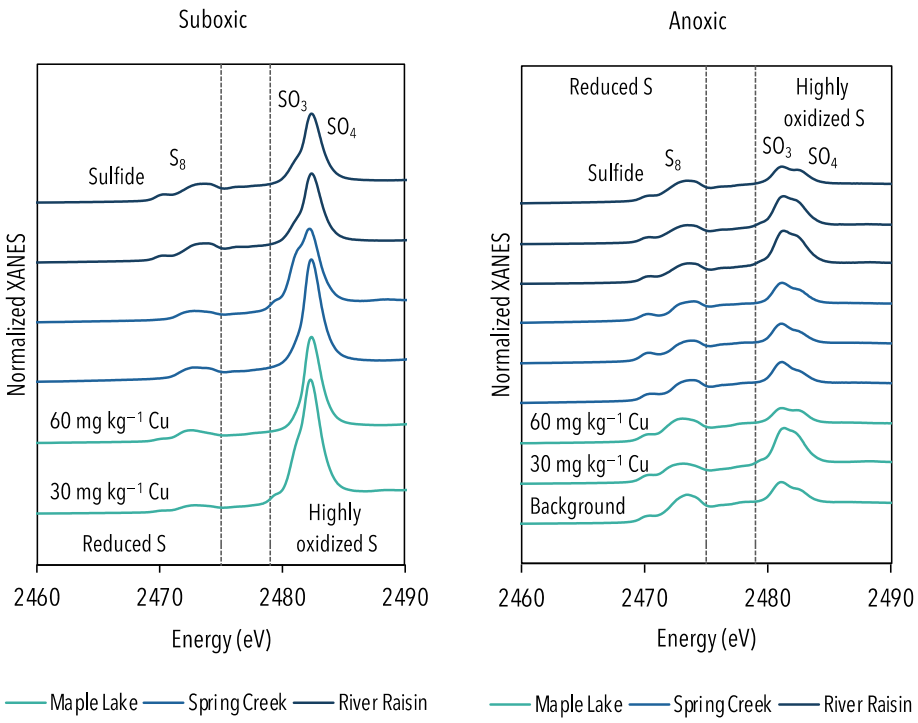

Fig. 3. Sulfur XANES spectra of Maple Lake, Spring Creek, and River Raisin sediments at background and Cu-spiked concentrations (30 and 60 mg kg^{-1}) without (left panel) and with (right panel) OM amendments.

Although S functional groups were similar between both treatments, their proportions changed significantly. Inorganic sulfides were observed in only two suboxic samples (River Raisin 30 mg kg^{-1} and 60 mg kg^{-1}), compared to the ubiquitous inorganic sulfide presence among the anoxic sediments. The position of the maximum for the oxidized sulfur peak (ester sulfates, inorganic sulfates, and sulfonates) shifted approximately −1 eV with increasing OC content and decreasing O_2 availability, indicating sulfate reduction had occurred, leaving only the organic oxidized S species (ester sulfates and sulfonates) and resulting in a decrease in the overall oxidation states.

3.4. Characterization of Cu species

In all anoxic sediment samples, Cu was predominantly present as Cu (I) coordinated to S. The X-ray absorption edges of the samples were all rather close to those of CuS and to the other Cu(I) compounds (Fig. 4; Figure S2), showing that a large part of the added Cu had been reduced to Cu(I) and then probably coordinated to S.

Linear combination fitting (LCF) of the XANES spectra (Table 5) confirmed CuS, or a similar phase, to be predominant in all anoxic samples except for Spring Creek 30 mg kg^{-1}, where Cu(I) complexed to OM thiols was suggested to be predominant. Further, LCF indicated that between 10 and 20% of the Cu remained as Cu(II) complexed to OM, as evidenced by the presence of the Cu(II)-HA standard (Cu^{2+} complexed to humic acid, c.f. Table S1) in the best fits.

Despite the LCF results, the EXAFS spectra visually did not show an obvious close correspondence to the CuS standard (Fig. 5A), as many samples lacked the extra shoulder at ~6.3 Å^{-1} for CuS in the EXAFS function. In fact, visual inspection suggested that the EXAFS of these samples seemed more related to copper(I) sulfide (Cu_2S). EXAFS shell fitting of the first shell revealed that Cu was predominantly coordinated to S in all anoxic samples, with a Cu–S distance of ~2.3 Å, which is similar to both CuS and Cu_2S, although clearly longer than what was obtained for the Cu(I)-thiol standard (2.24 Å, Table 5, Fig. 5B). For Spring Creek 30 mg kg^{-1}, however, shell fitting revealed the likely presence also of a minor fraction of oxygen atoms in the first shell, with a

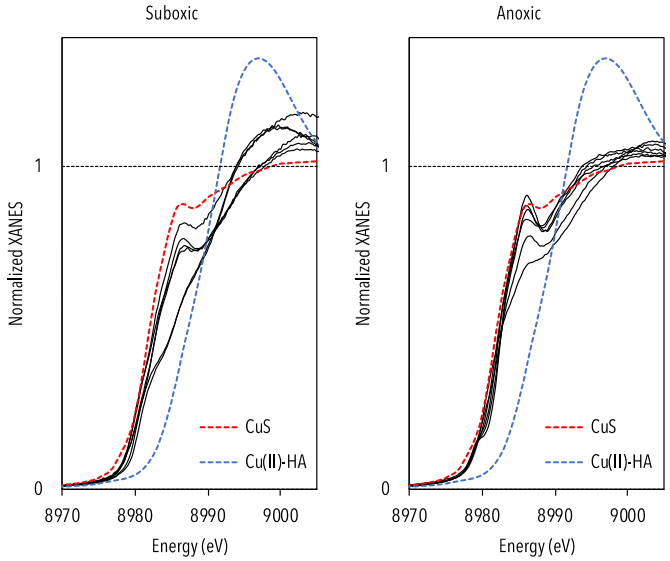

Fig. 4. Normalized Cu K-edge XANES spectra for all samples. The XANES spectra of CuS (red dashed line) and of Cu(II) complexed to humic acid (blue dashed line) are shown for comparison. (For interpretation of the references to colour in this figure legend, the reader is referred to the Web version of this article.)

distance (1.92 Å) similar to that expected for the four equatorial oxygens of a distorted Cu(II)–O octahedron.

Also, for the suboxic samples both the XANES and EXAFS results showed that Cu had been reduced in part to Cu(I) and coordinated to S, despite the lower occurrence of reduced S in these samples. For the Raisin River and the Maple Lake samples, there was even a predominance of Cu sulfides, similar to what was observed for the anoxic samples, and LCF indicated only around 20% persisted as Cu(II), all of which was complexed to OM. EXAFS shell fitting revealed only Cu–S at 2.27 Å

Table 5
Copper speciation as evidenced from Linear Combination Fitting (LCF) of XANES spectra. Results of the best fits are shown as %, with standard deviations within parenthesis. The sum of the percentages was not constrained to 100.

Sample	*Cu(I)*			*Cu(II)*		R factor
	CuS	Cu(I)-thiol	CuCl	CuO	Cu(II)-HA	
Anoxic						
Maple Lake 60 mg kg^{-1} Cu	83(2)			16 (2)		0.006
Maple Lake 30 mg kg^{-1} Cu	74(7)	5(7)			18(1)	0.007
Raisin River 60 mg kg^{-1} Cu	73(6)		10 (5)	18 (1)		0.003
Raisin River 30 mg kg^{-1} Cu	82(2)			11 (6)	6(5)	0.003
Spring Creek 60 mg kg^{-1} Cu	89(1)				10(1)	0.001
Spring Creek 30 mg kg^{-1} Cu	16(9)	60(10)			20(1)	0.013
Suboxic						
Maple Lake 60 mg kg^{-1} Cu	76(1)				19(1)	0.008
Maple Lake 30 mg kg^{-1} Cu	34 (10)	43(10)			20(1)	0.013
Raisin River 60 mg kg^{-1} Cu	57(8)	17(8)			22(1)	0.009
Raisin River 30 mg kg^{-1} Cu	63(8)	20(9)			22(1)	0.009
Spring Creek 60 mg kg^{-1} Cu	3(7)	44(7)			50(1)	0.006
Spring Creek 30 mg kg^{-1} Cu		49(1)			48(1)	0.008

in the first shell.

For Spring Creek samples, however, there was significant additional involvement of oxygen-bound Cu(II) in the first shell. In terms of the energy position at the absorption edge, these two samples were intermediate to those of the CuS and Cu(II)-HA standards, which can be seen in Fig. 6. The LCF suggested around 40–50% of the Cu to be present as Cu(I) complexed to thiols, the remainder being organically complexed Cu(II) (Table 5). EXAFS shell fitting showed a similar distribution between Cu(I)–S and Cu(II)–O paths in the first shell (Table 6). The mixture between Cu(I)–S and Cu(II)–O paths caused relatively flat and featureless EXAFS functions as well as FT magnitudes (Fig. 6A and B).

3.5. Raman and SEM/EDS spectroscopy

Fig. 6 shows the surface morphology and elemental analysis (SEM/EDS) as well as the mineralogical analysis (Raman) of the Cu-spiked sediments under suboxic and anoxic conditions. The EDS analysis of sediments under anoxic conditions (Fig. 6B and D) revealed an increase in carbon counts as a result of OM amendments. The images also evidenced the formation of regularly shaped CuS and FeS nanoparticles of less than 10 up to 20 μm under anoxic conditions.

The Raman spectra confirmed the previous results, indicating that all sediment samples were dominated by quartz, Fe and Cu sulfides, and S, whereas a few spots were consistent with amorphous material (Fig. 6E and F). Raman bands in quartz crystal at 207 and 128 cm^{-1} are characteristic of lattice modes whereas the strong peak at 470 cm^{-1} is characteristic of symmetric stretching vibration. The modes below 400 cm^{-1} are associated with the external modes of the ions (lattice phonons) and the internal modes of the Cu complex. The modes above 400 cm^{-1} are associated with the intramolecular vibration of sulfate.

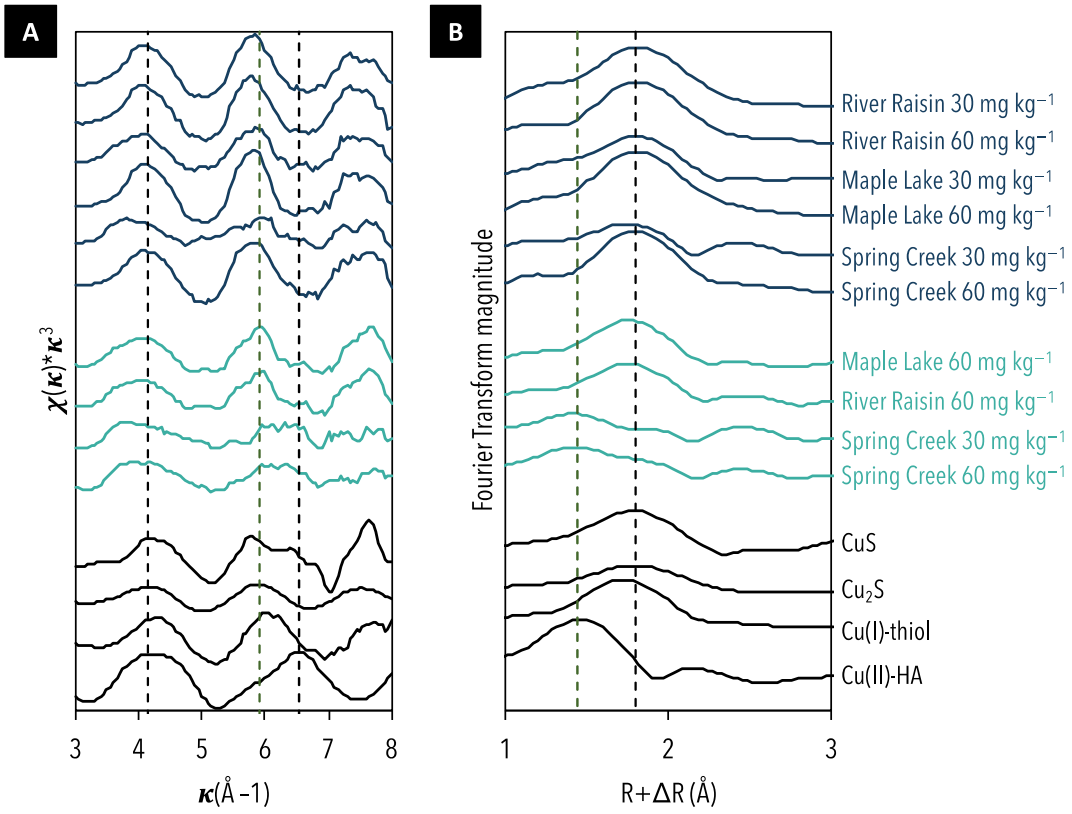

Fig. 5. k3-weighted (A) and Fourier Transform (B) magnitudes of Cu K-edge EXAFS spectra. The uppermost six spectra (dark blue lines) are anoxic samples, whereas the four spectra in the middle (light blue lines) are suboxic samples, and the four lowermost samples (black lines) are selected standards. Dashed lines at k = 4.15 $Å^{-1}$ and 5.9 $Å^{-1}$ denote Cu(I)–S interactions in Cu_2S, whereas the line at 6.55 $Å^{-1}$ denotes a Cu(II)–O interaction in Cu(II)-HA. The vertical dashed lines at R+ΔR = 1.44 Å and 1.8 Å indicate the first-shell distances of Cu(II)–O (1.94 Å) and Cu(I)–S (2.3 Å), respectively. (For interpretation of the references to colour in this figure legend, the reader is referred to the Web version of this article.)

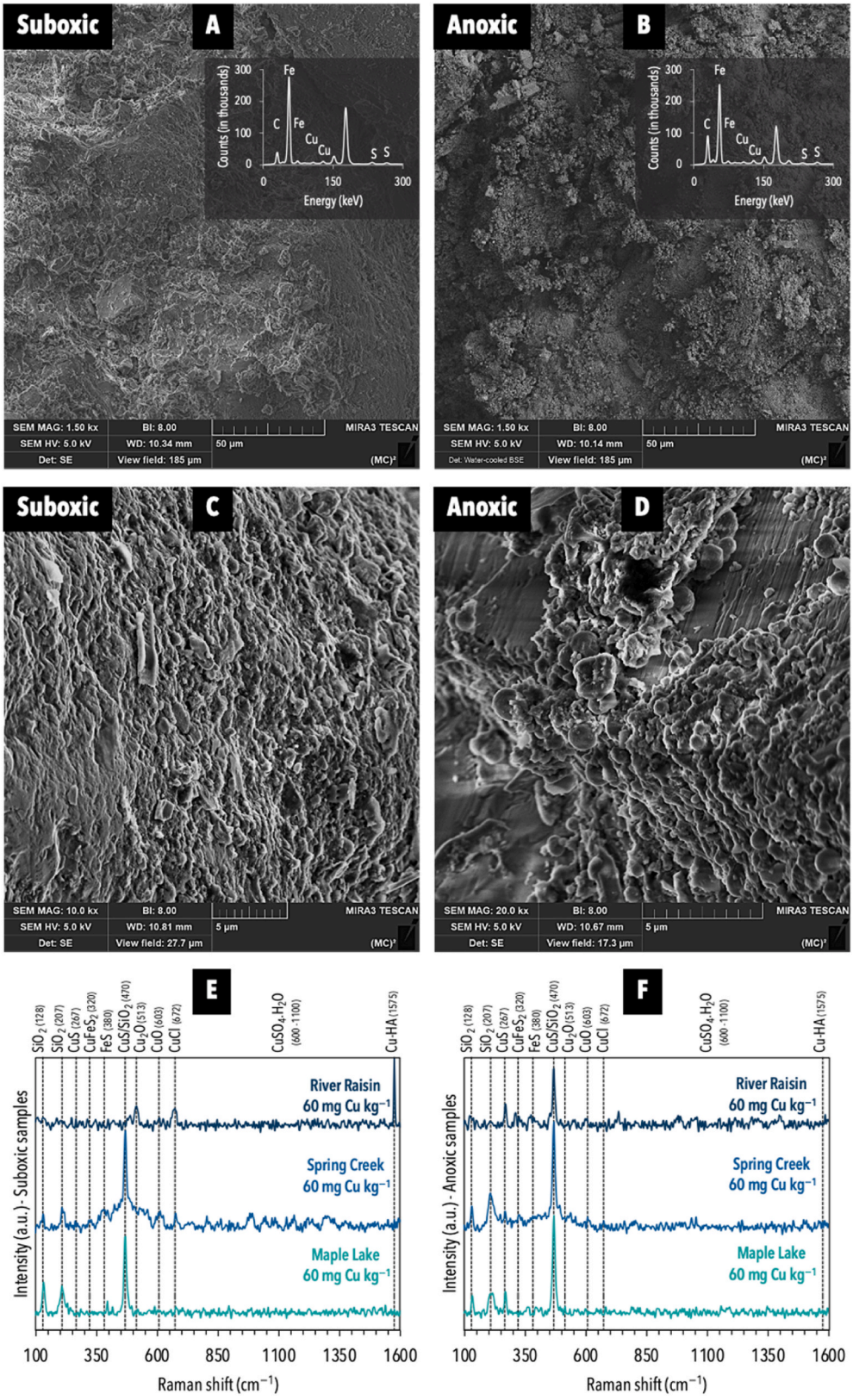

Fig. 6. Surface morphology (EDS/SEM) and elemental analysis (Raman spectroscopy) of the Cu-spiked sediments under suboxic and anoxic conditions.

Under anoxic conditions, Cu was reduced in part to Cu(I) and coordinated to S and possibly Fe. Raman peaks typically indicated the formation of Fe sulfides (FeS and FeS_2), Cu sulfides (covellite) and copper iron sulfides (chalcopyrite). The Raman spectrum of pyrite coincides with published data (Vogt et al., 1983; Kleppe and Jephcoat, 2004). The moderate 343 cm^{-1} and 380 cm^{-1} peaks represent Eg and Ag modes of pyrite; the weak 430 cm^{-1} peak is the Tg(3) mode of pyrite, respectively, and the 352 cm^{-1} peak is an overlap of pyrite [Tg(1), ~350 cm^{-1}] and quartz [A1, ~353 cm^{-1}]. As the Tg(2) mode of pyrite is weak and occurs $\leq$2 cm^{-1} apart from the intense Ag peak (Vogt et al., 1983) only the 343

Table 6
Summary of first-shell fit results: Cu K edge EXAFS spectra of samples and standards. Parameters in italics were constrained during fitting.

	Cu–O path			Cu–S path			ΔE (eV)	R factor
	CN[a]	R[a] (Å)	σ^2 (Å^2)	CN	R (Å)	σ^2 (Å^2)		
Anoxic								
ML 60 mg kg^{-1} Cu				4.2 (6)	2.33 (1)	0.008 (2)	−0.7 (1.2)	0.007
ML 30 mg kg^{-1} Cu				2.9 (2)	2.32 (1)	0.008 (1)	−4.1 (9)	0.020
RR 60 mg kg^{-1} Cu				3.6 (6)	2.33 (2)	0.007 (3)	−1.0 (1.6)	0.012
RR 30 mg kg^{-1} Cu				4.0 (6)	2.33 (1)	0.009 (3)	−0.8 (1.5)	0.009
SC 60 mg kg^{-1} Cu				3.1 (4)	2.31 (1)	0.006 (2)	−1.6 (1.2)	0.007
SC 30 mg kg^{-1} Cu	0.5 (3)	*1.92*	*0.005*	1.8 (3)	2.31 (2)	*0.007*	−7.1 (2.0)	0.025
Suboxic								
ML 60 mg kg^{-1} Cu				2.7 (3)	2.29 (1)	0.007 (2)	−5.0 (1.2)	0.005
RR 60 mg kg^{-1} Cu				2.9 (5)	2.29 (2)	0.009 (3)	−5.4 (1.8)	0.011
SC 60 mg kg^{-1} Cu	1.5 (1)	1.92 (1)	*0.005*	1.0 (1)	*2.30*	*0.007*	−4.7 (0.5)	0.003
SC 30 mg kg^{-1} Cu	1.5 (4)	1.91 (5)	*0.005*	0.7 (4)	2.33 (1)	*0.007*	−6.0 (5.0)	0.022
Selected standards								
CuS				2.2 (4)	2.27 (2)	0.006 (3)	−1.3 (1.6)	0.010
Cu_2S				1.5 (3)	2.31 (2)	0.007 (2)	−1.4 (1.6)	0.009
Cu(I)-thiol				2.4 (4)	2.24 (2)	0.006 (2)	−2.9 (1.8)	0.011
Cu(II)-HA	3.5 (3)	1.93 (1)	0.005 (2)					0.006

[a] CN = coordination number, R = atomic distance, σ^2 = Debye-Waller factor, ΔE = energy shift parameter, R factor = Athena goodness-of-fit parameter. Uncertainties of fitted parameters as given in Artemis (Ravel and Newville, 2005).

cm^{-1} and 379 cm^{-1} peaks of pyrite and the 465 cm^{-1} peak of quartz were fitted in this study.

Small amounts of Cu oxides and CuCl dihydrate (used during spiking procedures) were indicated in River Raisin and Spring Creek sediments under suboxic conditions, as identified by their Raman peaks at 603 and 672 cm^{-1}, respectively (Fig. 6E). Raman peaks belonging to Cu oxides had disappeared after OM amendments in River Raisin 60 mg kg^{-1}. This is consistent with the idea that with the addition of OM, Cu sulfides precipitate. Likewise, when comparing the anoxic with the suboxic sediments, we noticed a dramatic decrease of sulfates (especially in Spring Creek 60 mg kg^{-1}) and a simultaneous increase of sulfides.

A summary of Raman transitions for identification of the corresponding S_n^{2-}/S_0 species is provided in Table 7. The peak at 320 cm^{-1} has been assigned to the ν_2 mode of chalcopyrite (Parker et al., 2008). Except for Raisin River 60 mg kg^{-1}, covellite was identified in all sediment samples and consists of a symmetric S–S (ν_{SS}) stretching band at 470 cm^{-1} and a smaller band at 267 cm^{-1}, attributed to lattice vibrations (Parker et al., 2008). Elemental octasulfur (S_8) also yields a strong ν_{SS} band at 470 cm^{-1} (Eckert and Steudel, 2003). However, S_8 displays a band from S–S–S (δ_{SSS}) chain bending at ~208 cm^{-1} which is not found in covellite (Mycroft et al., 1990).

3.6. Effects of anoxic conditions on Cu toxicity

Table 8 shows mean acute and chronic toxicity to *H. azteca* and *D. magna* (sediment and overlying water, respectively) for background and Cu-spiked (30 and 60 mg kg^{-1}) sediments. *H. azteca* and *D. magna* met the minimum acceptable performance criteria (survival >80%) in the controls. There were no significant differences in survival between the background and spiked sediments apart from the fact that *D. magna* had lower survival in Spring Creek sediments spiked with 30 and 60 mg kg^{-1} compared to the control ($p < 0.05$). This may have been due to higher bioavailable Cu concentrations. Additionally, there was a significant increase in *H. azteca* survival ($p = 0.03$) and growth ($p < 0.0001$) after OM amendment compared to non-amended samples.

4. Discussion

The addition of OM triggered a shift from suboxic to anoxic conditions, followed by a rapid decline in redox potential and an increase in pH in the amended sediments. This suggests that the added OM was decomposed, with subsequent consumption of oxygen and consumption of other terminal electron acceptors (e.g., nitrate, Mn(IV), Fe(III), sulfate, carbon dioxide) (Borch et al., 2009).

The OM addition stimulates an increase in pH because anerobic processes are associated with many microbial groups that are heterotrophs (Johnson and Hallberg, 2005). The relative importance of different reduction processes associated with pH increase depends on several factors, including initial pH, redox potential, and the concentrations of various electron acceptors (Yuan et al., 2015). Sulfate and iron reduction processes are likely strong contributors to pH increases in sulfidic sediments, similar to the sediments used in this study with the amended treatments (Jayalath et al., 2016). Decomposition of OM and associated decarboxylation of organic acid anions can also result in pH increase (Yan et al., 1996).

Overall, the percentage of OC decreased with increasing spiked Cu concentrations in this study, suggesting that the presence of added Cu elicited its consumption by stressed microorganisms (Dupont et al., 2011). In the anoxic samples, most of the sulfate had been reduced,

Table 7
Summary of Raman transitions identification in terms of main sulfur and copper-sulfide phases on suboxic and anoxic sediment samples.

Species	Raman peak positions	References
Chalcopyrite (monosulfide, S_2^{2-})	292 (ν1), 320 (ν3), 471 (ν2)	Parker et al. (2008)
Polysulfides (S_n^{2-})	From 443 to 480, main at 470 (ν1)	Mycroft et al. (1990)
Elemental sulfur (S_8)	Main at 150 (ν3), 220 (ν2), and 470 (ν1)	Eckert and Steudel (2003)
Covellite (S^-)	267 (ν2), 471 (ν1)	Parker et al. (2008)
Pyrite (FeS_2)	344 (ν2), 380 (ν1), and 430 (ν3)	Vogt et al. (1983), Kleppe and Jephcoat (2004)
Copper chloride dihydrate ($CuCl_2 \times 2H_2O$)	672	Frost et al. (2003)
Copper oxides (Cu_2O, CuO)	513, 603	El Jaroudi et al. (2000)
Copper sulfates ($CuSO_4 \times H_2O$)	From 600 to 1500	Parker et al. (2008)

Table 8
Mean acute and chronic toxicity to *Hyalella azteca* and *Daphnia magna* in sediment and overlying water for background and Cu-spiked (30 and 60 mg kg^{-1}) sediments (±SD). Laboratory ion-enriched water (IEW) was used as the control.

Sample	Treatment	*H. azteca* survival (%)	*H. azteca* IGR (μg day^{-1})	*D. magna* survival (%)	*D. magna* IGR (μg day^{-1})	*D. magna* R_0 (neonates $adults^{-1}$)
Anoxic						
Control	IEW	100 ± 0.0 a	4.5 ± 0.2 a	100 ± 0.0 a	45.5 ± 6.0 a	4.8 ± 0.6 a
Maple	Background	95.0 ± 5.0 a	4.4 ± 0.2 a	100 ± 0.0 a	43.0 ± 6.0 a	4.6 ± 0.5 a
Lake	30 mg kg^{-1} Cu	95.0 ± 5.0 a	4.5 ± 0.2 a	90.0 ± 10.0 a	44.8 ± 6.2 a	5.3 ± 0.5 a
	60 mg kg^{-1} Cu	90.0 ± 7.1 a	4.5 ± 0.2 a	87.5 ± 8.3 a	42.4 ± 2.0 a	5.6 ± 0.8 a
River	Background	100 ± 0.0 a	4.6 ± 0.3 a	100 ± 0.0 a	45.2 ± 6.0 a	5.0 ± 0.3 a
Raisin	30 mg kg^{-1} Cu	97.5 ± 4.3 a	4.4 ± 0.1 a	95.0 ± 5.0 a	45.6 ± 7.3 a	5.4 ± 0.5 a
	60 mg kg^{-1} Cu	97.5 ± 4.3 a	4.5 ± 0.3 a	87.5 ± 4.3 a	47.4 ± 4.4 a	5.6 ± 0.4 a
Spring	Background	100 ± 0.0 a	4.2 ± 0.1 a	100 ± 0.0 a	44.9 ± 2.9 a	4.5 ± 0.4 a
Creek	30 mg kg^{-1} Cu	95.0 ± 5.0 a	4.6 ± 0.3 a	92.5 ± 8.3 a	49.5 ± 3.1 a	4.9 ± 0.4 a
	60 mg kg^{-1} Cu	90.0 ± 0.0 a	4.6 ± 0.2 a	85.0 ± 5.0 a	46.4 ± 2.9 a	5.7 ± 0.4 a
Pr > F(Model)		0.001	0.023	0.481	0.004	0.855
Significant		Yes	Yes	No	Yes	No
Suboxic						
Control	IEW	97.5 ± 4.3 a	4.0 ± 0.1 a	100 ± 0.0 a	39.0 ± 2.8 a	4.6 ± 0.6 a
Maple	Background	97.5 ± 4.3 a	4.0 ± 0.1 a	100 ± 0.0 a	43.1 ± 2.1 a	4.6 ± 0.6 a
Lake	30 mg kg^{-1} Cu	95.0 ± 5.0 a	4.0 ± 0.1 a	90.0 ± 7.1 abc	39.5 ± 5.8 a	4.5 ± 0.6 a
	60 mg kg^{-1} Cu	87.5 ± 4.3 ab	3.3 ± 0.2 c	82.5 ± 4.3 bc	39.0 ± 3.3 a	4.4 ± 0.4 a
River	Background	97.5 ± 4.3 a	3.9 ± 0.1 ab	95.0 ± 8.7 ab	42.8 ± 1.6 a	5.2 ± 1.0 a
Raisin	30 mg kg^{-1} Cu	95.0 ± 8.6 a	4.0 ± 0.2 a	90.0 ± 7.1 abc	43.3 ± 1.4 a	4.4 ± 0.2 a
	60 mg kg^{-1} Cu	92.5 ± 8.2 a	4.0 ± 0.2 a	82.5 ± 4.3 bc	37.4 ± 4.2 ab	4.4 ± 0.2 a
Spring	Background	100 ± 0.0 a	4.0 ± 0.1 a	100 ± 0.0 a	42.5 ± 1.4 a	4.1 ± 0.5 a
Creek	30 mg kg^{-1} Cu	82.5 ± 10.8 ab	3.2 ± 0.1 c	80.0 ± 7.1 c	35.1 ± 4.0 ab	5.0 ± 0.3 a
	60 mg kg^{-1} Cu	72.5 ± 10.8 b	2.7 ± 0.1 d	80.0 ± 0.0 c	28.5 ± 2.5 b	4.4 ± 0.3 a
Pr > F(Model)		0.001	<0.0001	<0.0001	0.000	0.293
Significant		Yes	Yes	Yes	Yes	No

increasing the fraction of reduced S species considerably. Organic matter is required by sulfate reducing bacteria that use it as an energy source (Thiel et al., 2019). Hence, the anoxic samples had a larger concentration of both inorganic sulfide and thiolated organic compounds, with which spiked Cu could react.

Sequential extractions suggested that, in the absence of OM, Cu was present mainly in the reducible fraction in the Spring Creek and Maple Lake sediments, which shows that Cu was relatively soluble and to a significant extent surface-bound in e.g., OM complexes. The relatively low TOC and AVS levels at both sites may have been limiting factors for substantial sulfate reduction and Cu sulfide mineral formation, as indicated by the BCR-701 analysis. Moreover, Spring Creek sediment is comprised by medium to coarse particles. Compared to sandy sediments, silt and clay particles have larger specific surface areas (Rojas and Silva, 2005; Álvarez-Iglesias and Rubio, 2012), and the surfaces of fine-grained sediments are more often coated by an OM layer (Mirlean et al., 2020). Hence, fine-grained sediments often have more associated OM than coarser sediments (Quintana et al., 2020). Organic coatings on fine sediments provide an important substrate for bacterial activity and stimulate oxygen and sulfate consumption, which favors a decrease in redox potential and enhances dissolved sulfide production (Jørgensen and Kasten, 2005; Bianchi, 2007).

Although TOC levels did not increase significantly after OM amendments, it favored oxygen depletion (DO concentration < 1 μM) and substantially affected Cu partitioning in the microcosms. Under anoxic conditions, Cu from the exchangeable/acid soluble and reducible fractions (F1 + F2) was repartitioned into the more recalcitrant oxidizable Cu fraction. The transformations and fluxes of Cu between various compartments in the aquatic environment are associated with Cu's strong tendency to bind to various dissolved ligands and solid phases (Rader et al., 2019). The reduction of Cu(II) to Cu(I) may have been proceeded by microbial reduction or abiotic processes, such as Cu (II) reduction by dissolved Fe^{2+} (Matocha et al., 2005) or natural OM (Pham et al., 2012). For example, Simpson et al. (2000) emphasized the importance of FeS as the most reactive phase in anoxic sulfidic sediments that results in reduction of Cu(II) by Fe(II) and subsequent formation of Cu_2S.

The results of X-ray absorption spectroscopy clearly showed reduction of Cu(II) within the 28 days of incubation for all systems, both suboxic and anoxic. However, the extent of Cu(II) reduction was more complete in the OM-amended systems. At the end, Cu was predominantly present as Cu(I) bound to sulfide, with the exception of the suboxic Spring Creek sediments, where about half of the Cu remained as Cu(II) complexed to OM. The exact nature of the Cu-sulfide phases is not completely clear, because the XANES and EXAFS results are not fully consistent; the XANES suggests important roles of CuS and organically complexed Cu(I) (Cu(I)-thiol), whereas the EXAFS results are in better agreement with an important role of Cu_2S. There might be different explanations for this discrepancy. First, it is possible that the samples contained a mix of poorly defined amorphous Cu_xS_y phases, which may partly have crystallized to CuS, and of Cu(I) bound to thiols. Second, there may also be other Cu–S phases present, for example chalcopyrite, for which the XAS spectra were not available to us. The XANES spectrum of chalcopyrite has some similarities to some of our samples (particularly some of the anoxic ones), and it is not very different from the CuS standard, as judged from spectra presented by Pattrick et al. (1997) and Yang et al. (2013). Therefore, the exact composition of the Cu sulfides formed remains uncertain.

Without significant quantities of biogenic sulfide, Cu(I) may have been stabilized against disproportionation with complexation by reduced organic S groups of bacterial cell surfaces, extracellular polymeric substances (EPS) or OM. Many studies have shown that thiol-containing compounds (e.g., glutathione) have an important role in the stabilization of Cu(I) in estuarine systems (Jeppe et al., 2017). The fact that there is considerable variation in the XANES spectra further suggests that the exact composition of the Cu(I)–S phases was not the same in the samples.

The initial formation of amorphous Cu_xS_y, and the slow crystallization to CuS (covellite) or to chalcopyrite is also in agreement with other recent studies in which the fate of Cu nanoparticles have been studied (Gogos et al. 2017, 2018). One may hypothesize, therefore, that with increasing time under anaerobic conditions the Cu speciation will be more clearly dominated by CuS or chalcopyrite – and that consequently the EXAFS spectra will gradually become increasingly consistent with one or both Cu sulfides.

Small amounts of Cu oxides were observed in River Raisin and Spring

Creek sediments under suboxic conditions, as indicated by Raman spectroscopy. During laboratory manipulations for Raman analysis, the sediment samples were placed in a stub and allowed to dry for a few minutes, possibly causing some oxidation. Under anoxic conditions, Cu had been reduced in part to Cu(I) and was coordinated to S and Fe. Raman peaks typically indicated the formation of Fe sulfides (FeS and FeS_2) and copper sulfides (covellite and chalcopyrite). This suggests that with the addition of OM, Cu sulfides precipitated following sulfate reduction, leading to desorption of Cu(I) from OM, and following the reduction of organically complexed Cu(II). Prior studies by McNeil et al. (1991) identified covellite (CuS) as the primary solid phase that results from biogenic Cu-sulfide formation in conditions with excess sulfide (Bilgin and Jaffé, 2019).

Sulfide precipitation greatly reduced Cu toxicity. *H. azteca* and *D. magna* survival in anoxic treatments were significantly higher ($p = 0.001$), with mean amphipod survival increasing by 17.5% relative to suboxic conditions in Spring Creek sediments amended with 60 mg kg^{-1} Cu. *D. magna* had lower survival in Spring Creek sediments spiked with 30 and 60 mg kg^{-1} compared to the control ($p < 0.05$). This may have been due to higher bioavailable Cu in the coarse sediments with low AVS availability.

There was also a significant increase in *H. azteca* growth ($p < 0.0001$) in all unamended sediments compared to non-amended treatments. Most organisms – including *H. azteca* – live in oxic surface sediments or in oxygenated microenvironments that form in suboxic and anoxic sediments (e.g., by irrigation with oxygen-containing waters). The CuS formation in these environments is key to mitigating Cu bioavailability and toxicity (Di Toro et al., 2001b; Rader et al., 2019). It is possible that benthic invertebrates may also ingest large amounts of sediment while foraging for food, and some species may have exposure to ingested labile metals with toxic effects (Casado-Martinez et al., 2010).

Studies of caged *H. azteca* and indigenous colonies of benthic macroinvertebrates showed no toxic effects in metal-spiked sediments as metals were partitioned out quickly, unless concentrations exceeded AVS and Fe oxide binding thresholds (Burton et al., 2005; Costello and Burton, 2014; Mendonca et al., 2017). Besser et al. (2003) conducted a study to evaluate effects of OM on the bioavailability and acute toxicity of Cd and Cu to *H. azteca* in two spiked sediments – one with purified cellulose and one with natural humus. The cellulose sediment had minimal effect on metal bioavailability and toxicity, likely due to the lack of chemical structures in cellulose for metal binding, such as carboxylic groups (Chapman et al., 1998). In contrast, natural humus reduced toxicity. Sediments with high levels of humus increased survival between 35 and 90% for both metals.

4.1. Implications for environmental risk assessment of copper

The diagenetic transformations of S have a significant role in the chemistry of freshwater sediments, significantly influencing copper speciation. We showed that OM amendments of Cu-spiked sediments enhance anoxic conditions, reducing highly oxidized S species. In the presence of S(-II), Cu(II) was reduced to Cu(I) and then precipitated with S(-I) to form Cu sulfide minerals, such as amorphous covellite, consequently reducing the mobility, bioavailability, and toxicity of Cu in sediments. This information may be useful in the context of environmental hazard and risk assessment of copper. Similar transformations were also observed under suboxic conditions and without OM amendments. However, low AVS, particle size, and OC appear to be limiting factors for sulfate reductions in some sediments, and in those cases most of the Cu predominated as OM-bound Cu(I) and Cu(II) under suboxic conditions.

Credit author statement

E.C. Cervi: Conceptualization, Methodology, Investigation, Resources, Data curation, Writing – original draft, S. Clark: Formal analysis (XANES), Investigation, Data curation, Writing – original draft, K.E. Boye: Formal analysis (XANES), Resources (SSRL), J.P. Gustafsson: Methodology, Formal analysis (EXAFS), Funding acquisition (SSRL), Writing – review & editing, S. Baken: Supervision, Project administration, Writing – review & editing, G.A. Burton, Jr.: Methodology, Supervision, Project administration, Funding acquisition (European Copper Institute), Writing – review & editing

Declaration of competing interest

The authors declare that they have no known competing financial interests or personal relationships that could have appeared to influence the work reported in this paper.

Acknowledgments

This research was financed by the European Copper Institute. The authors acknowledge the technical support from Dr. Nancy S. Muyanja (Michigan Center for Materials Characterization, University of Michigan, Ann Arbor, US) for SEM/EDS and Raman spectroscopy analysis. Ruben Kretzschmar, Henric Lassesson and Charlotta Tiberg are acknowledged for sharing Cu K-edge XAS spectra of the Cu standards detailed in Table S1, Supplemental data. Use of the Stanford Synchrotron Radiation Lightsource - SSRL, SLAC National Accelerator Laboratory, is supported by the U.S. Department of Energy, Office of Science, Office of Basic Energy Sciences under Contract No. DE-AC02-76SF00515. The SSRL Structural Molecular Biology Program is supported by the DOE Office of Biological and Environmental Research, and by the National Institutes of Health - NIH, National Institute of General Medical Sciences – NIGMS (P30GM133894). The contents of this publication are solely the responsibility of the authors and do not necessarily represent the official views of NIGMS or NIH. Work by K. Boye was supported through the SLAC Floodplain Hydro-Biogeochemistry SFA program of the US Department of Energy, Office of Biological and Environmental Research, Environmental System Science division, under DOE contract no. DE-AC0276SF00515SBR.

References

Ahlf, W., Drost, W., Heise, S., 2009. Incorporation of metal bioavailability into regulatory frameworks—metal exposure in water and sediment. J. Soils Sediments 9, 411–419. https://doi.org/10.1007/s11368-009-0109-6.

Almkvist, G., Boye, K., Persson, I., 2010. K-edge XANES analysis of sulfur compounds:an investigation of the relative intensities using internal calibration. J. Synchrotron Radiat. 17, 683–688.

Álvarez-Iglesias, P., Rubio, B., 2012. Early diagenesis of organic-matter-rich sediments in a ría environment: organic matter sources, pyrites morphology and limitation of pyritization at depth Estuarine. Coast. Shelf Sci. 100, 113–123.

Besser, J.M., Brumbaugh, W.G., May, T.W., Ingersoll, C.G., 2003. Effects of organic amendments on the toxicity and bioavailability of cadmium and copper in spiked formulated sediments. Environ. Toxicol. Chem. 22, 805–815.

Bianchi, T., 2007. Biogeochemistry of Estuaries. Oxford University Press, Oxford.

Bilgin, A., Jaffé, P.R., 2019. Precipitation of copper (II) in a two-stage continuous treatment system using sulfate reducing bacteria. Waste Biomass Valor 10, 2907–2914. https://doi.org/10.1007/s12649-018-0329-3.

Borch, T., Kretzschmar, R., Kappler, A., Cappellen, P.V., Ginder-Vogel, M., Voegelin, A., Campbell, K., 2009. Biogeochemical redox processes and their impact on contaminant dynamics. Environ. Sci. Technol. 44, 15–23.

Boye, K., Almkvist, G., Nilsson, S.I., Eriksen, J., Persson, I., 2011. Quantification of chemical sulphur species in bulk soil and organic sulphur fractions by S K-edge XANES spectroscopy. Eur. J. Soil Sci. 62, 874–881.

Burton Jr., G.A., Nguyen, L.T.H., Janssen, C., Baudo, R., McWilliam, R., Bossuyt, B., Beltrami, M., Green, A., 2005. Field validation of sediment zinc toxicity. Environ. Toxicol. Chem. 24, 541–553.

Burton, G.A., Green, A., Baudo, R., Forbes, V., Nguyen, L.T., Janssen, C.R., Kukkonen, J., Leppanen, M., Maltby, L., Soares, A., Kapo, K., Smith, P., Dunning, J., 2007. Characterizing sediment acid volatile sulfide concentrations in European streams. Environ. Toxicol. Chem. 26 (1), 1–12. https://doi.org/10.1897/05-708r.1.

Burton, G.A., Hudson, M.L., Huntsman, P., Carbonaro, R.F., Rader, K.J., Waeterschoot, H., Baken, S., Garman, E., 2019. Weight-of-evidence approach for assessing removal of metals from the water column for chronic environmental hazard classification. Environ. Toxicol. Chem. 38, 1839–1849.

Caetano, M., Madureira, M.J., Vale, C., 2003. Metal remobilisation during resuspension of anoxic contaminated sediment: short-term laboratory study. Water Air Soil Pollut. 143, 23–40.
Campana, O., Simpson, S.L., Spadaro, D.A., Blasco, J., 2012. Sub-lethal effects of copper to benthic invertebrates explained by sediment properties and dietary exposure. Environ. Sci. Technol. 46, 6835–6842.
Cantwell, M.G., Burgess, R.M., King, J.W., 2008. Resuspension of contaminated field and formulated reference sediments part I: evaluation of metal release under controlled laboratory conditions. Chemosphere 73, 1824–1831.
Casado-Martinez, M.C., Smith, B.D., Luoma, S.N., Rainbow, P.S., 2010. Metal toxicity in a sediment-dwelling polychaete: threshold body concentrations or overwhelming accumulation rates? Environ. Pollut. 158, 3071–3076.
Cervi, E.C., Thiamkeelakul, K., Hudson, M., Rentschler, A., Nedrich, S., Brown, S.S., Burton, G.A., 2020. Laboratory and field-based assessment of the effects of sediment capping materials on zinc flux, bioavailability, and toxicity. Environ. Toxicol. Chem. 39, 240–249.
Chapman, P.M., Wang, F., Janssen, C., Persoone, G., Allen, H.E., 1998. Ecotoxicology of metals in aquatic sediments: binding and release, bioavailability, risk assessment, and remediation. Can. J. Fish. Aquat. Sci. 55, 2221–2243.
Costello, D.M., Burton, G.A., 2014. Response of stream ecosystem function and structure to sediment metal: context-dependency and variation among endpoints. Elementa 2. DOI: 10.12952/journal.elementa.000030.
Costello, D.M., Hammerschmidt, C.R., Burton, G.A., 2015. Copper sediment toxicity and partitioning during oxidation in a flow-through flume. Environ. Sci. Technol. 49, 6926–6933.
Costello, D.M., Harrison, A.M., Hammerschmidt, C.R., Mendonca, R.M., Burton, G.A., 2019. Hitting reset on sediment toxicity: sediment homogenization alters the toxicity of metal-amended sediments. Environ. Toxicol. Chem. 38, 1995–2007. https://doi.org/10.1002/etc.4512.
Davutluoglu, O.I., Seckin, G., Ersu, C.B., Yilmaz, T., Sari, B., 2011. Heavy metal content and distribution in surface sediments of the Seyhan River, Turkey. J. Environ. Manag. 92, 2250–2259.
Di Toro, D.M., Allen, H.E., Bergman, H.L., Meyer, J.S., Paquin, P.R., Santore, R.C., 2001a. Biotic ligand model of the acute toxicity of metals. 1. Technical basis. Environ. Toxicol. Chem. 20, 2383–2396.
Di Toro, D.M., Kavvadas, C.D., Mathew, R., Paquin, P.R., Winfield, R.P., 2001b. The Persistence and Availability of Metals in Aquatic Environments. International Council on Metals and the Environment, Ottawa, ON, Canada.
Donner, E., Ryan, C.G., Howard, D.L., Zarcinas, B., Scheckel, K.G., McGrath, S.P., de Jonge, M.D., Paterson, D., Naidu, R., Lombi, E., 2012. A multi-technique investigation of copper and zinc distribution, speciation and potential bioavailability in biosolids. Environ. Pollut. 166, 57–64.
Dupont, C.L., Grass, G., Rensing, C., 2011. Copper toxicity and the origin of bacterial resistance—new insights and applications. Metallomics 3 (11), 1109–1118. https://doi.org/10.1039/c1mt00107h.
Eckert, B., Steudel, R., 2003. Molecular spectra of sulfur molecules and solid sulfur allotropes. Top. Curr. Chem. 231, 31–98.
El Jaroudi, O., Picquenard, E., Demortier, A., Lelieur, J.P., Corset, J., 2000. Polysulfide anions. II. Structure and vibrational spectra of the S_4^{2-} and S_5^{2-} anions. Influence of the cations on bond length, valence, and torsion angle. Inorg. Chem. 39, 2593–2603.
Evans, H.T., Konnert, J.A., 1976. Crystal structure refinement of covellite. Am. Mineral. 61, 996–1000.
Frost, R.L., Yang, J., Ding, Z., 2003. Raman and FTIR spectroscopy of natural oxalates: implications for the evidence of life on Mars. Chin. Sci. Bull. 48, 1844–1852.
Fukunaga, A., Anderson, M.J., 2011. Bioaccumulation of copper, lead and zinc by the bivalves *Macomona liliana* and *Austrovenus stutchburyi*. J. Exp. Mar. Biol. Ecol. 396, 244–252. https://doi.org/10.1016/j.jembe.2010.10.029.
Fulda, B., Voegelin, A., Ehlert, K., Kretzschmar, R., 2013a. Redox transformation, solid phase speciation and solution dynamics of copper during soil reduction and reoxidation as affected by sulfate availability. Geochem. Cosmochim. Acta 123, 385–402. https://doi.org/10.1016/j.gca.2013.07.017.
Fulda, B., Voegelin, A., Maurer, F., Christl, I., Kretzschmar, R., 2013b. Copper redox transformation and complexation by reduced and oxidized soil humic acid. 1. X-Ray absorption spectroscopy study. Environ. Sci. Technol. 47 (19), 10903–10911. https://doi.org/10.1021/es4024089.
Gardham, S., Hose, G.C., Simpson, S.L., Jarolimek, C., Chariton, A.A., 2014. Long-term copper partitioning of metal-spiked sediments used in outdoor mesocosms. Environ. Sci. Pollut. Res. 21, 7130–7139. https://doi.org/10.1007/s11356-014-2631-3.
Gogos, A., Thalmann, B., Voegelin, A., Kaegi, R., 2017. Sulfidation kinetics of copper oxide nanoparticles. Environ. Sci.: Nano 4, 1733–1741.
Gogos, A., Voegelin, A., Kaegi, R., 2018. Influence of organic compounds on the sulfidation of copper oxide nanoparticles. Environ. Sci.: Nano 5, 2560–2569.
Jayalath, N., Mosley, L.M., Fitzpatrick, R.W., Marschner, P., 2016. Addition of organic matter influences pH changes in reduced and oxidised acid sulfate soils. Geoderma 262, 125–132.
Jeppe, K.J., Yang, J.H., Long, S.M., Carew, M.E., Zhang, X.W., Pettigrove, V., Hoffmann, A.A., 2017. Detecting copper toxicity in sediments: from the sub individual level to the population level. J. Appl. Ecol. 54 (5), 1331–1342. https://doi.org/10.1111/1365-2664.12840.
Johnson, D.B., Hallberg, K.B., 2005. Acid mine drainage remediation options: a review. Sci. Total Environ. 338 (1–2), 3–14.
Jørgensen, B., Kasten, S., 2005. Sulfur cycling and methane oxidation. In: Schulz, H., Izabel, M. (Eds.), Marine Geochemistry. Springer, Berlin.
Karlsson, T., Persson, P., Skyllberg, U., 2006. Complexation of copper(II) in organic soils and in dissolved organic matter - EXAFS evidence for chelate ring structures. Environ. Sci. Technol. 40, 2623–2628.
Khangarot, B.S., Das, S., 2010. Effects of copper on the egg development and hatching of a freshwater pulmonate snail Lymnaea luteola L. J. Hazard Mater. 179, 665–675. https://doi.org/10.1016/j.jhazmat.2010.03.054.
Kleppe, A., Jephcoat, A., 2004. High-pressure Raman spectroscopic studies of FeS_2 pyrite. Mineral. Mag. 68, 433–441.
Luoma, S.N., Rainbow, P.S., 2008. Metal Contamination in Aquatic Environments: Science and Lateral Management. Cambridge Univ, Cambridge (UK), p. 573.
Luther, G.W., Theberge, S.M., Rozan, T.F., Rickard, D., Rowlands, C.C., Oldroyd, A., 2002. Aqueous copper sulfide clusters as intermediates during copper sulfide formation. Environ. Sci. Technol. 36, 394–402.
Matocha, C.J., Karathanasis, A.D., Rakshit, S., Wagner, K.M., 2005. Reduction of copper (II) by iron(II). J. Environ. Qual. 34, 1539–1546.
McNeil, M.B., Jones, J.M., Little, B.J., 1991. Mineralogical fingerprints for corrosion processes induced by sulfate reducing bacteria. NACE Ann. Conf. 580, 1–16.
Mendonca, R., Daley, J., Hudson, M., Schlekat, C., Burton, G.A., Costello, D., 2017. Metal oxides in surface sediment control nickel bioavailability to benthic macroinvertebrates. Environ. Sci. Technol. 51, 13407–13416.
Mirlean, N., Bem, A.L., Quintana, G.C.R., Costa, L.P., Ferraz, A.H., 2020. Sulfate reduction and alterability of sulfur species in sediments of an estuary with irregular hydrological regime. Ocean Coast. Res. 68 (e20321), 1–16. https://doi.org/10.1590/s2675-28242020068321.
Morse, J.W., Luther, G.W., 1999. Chemical influences on trace metal-sulfide interactions in anoxic sediments. Geochem. Cosmochim. Acta 63, 3373–3378.
Mycroft, J.R., Bancroft, G.M., McIntyre, N.S., Lorimer, J.W., Hill, I.R., 1990. Detection of sulfur and polysulfides on electrochemically oxidized pyrite surfaces by X-ray photoelectron spectroscopy and Raman spectroscopy. J. Electroanal. Chem. 292, 139–152.
Parker, G.K., Woods, R., Hope, G.A., 2008. Raman investigation of chalcopyrite oxidation. Colloid. Surface. Physicochem. Eng. Aspect. 318, 160–168.
Pattrick, R.A.D., Mosselmans, J.F.W., Charnock, J.M., England, K.E.R., Helz, G.R., Garner, C.D., Vaughan, D.J., 1997. The structure of amorphous copper sulfide precipitates: an X-ray absorption study. Geochem. Cosmochim. Acta 61, 2023–2036.
Pham, A.N., Rose, A.L., Waite, T.D., 2012. Kinetics of Cu(II) reduction by natural organic matter. J. Phys. Chem. 116, 6590–6599.
Quintana, G., Mirlean, N., Costa, L., Johannesson, K., 2020. Mercury distributions in sediments of an estuary subject to anthropogenic hydrodynamic alterations (Patos Estuary, Southern Brazil). Environ. Monit. Assess. 192 (5), 1–12. https://doi.org/10.1007/s10661-020-8232-3.
Rader, K.J., Carbonaro, R.F., van Hullebusch, E.D., Baken, S., Delbeke, K., 2019. The fate of copper added to surface water: field and modeling studies. Environ. Toxicol. Chem. 38, 1386–1399.
Rauret, G., López-Sánchez, J.F., Lück, D., Yli-Halla, M., Muntau, H., Quevauviller, P., 2001. The Certification of the Extractable Contents (Mass Fractions) of Cd, Cr, Cu, Ni, Pb and Zn in a Freshwater Sediment Following a Sequential Extraction Procedure. BCR-701. BCR Information. Reference Materials Report EUR 19775 EN.
Ravel, B., Newville, M., 2005. ATHENA, artemis, hephaestus: data analysis for X-ray absorption spectroscopy using IFEFFIT. J. Synchrotron Radiat. 12, 537–541.
Rojas, N., Silva, N., 2005. Early diagenesis and vertical distribution of organic carbon and total nitrogen in recent sediments from southern Chilean fjords (Boca del Guafo to Pulluche Channel). Invest. Mar. 33, 183–194.
Roman, Y.E., De Schamphelaere, K.A.C., Nguyen, L.T.H., Janssen, C.R., 2007. Chronic toxicity of copper to five benthic invertebrates in laboratory-formulated sediment: sensitivity comparison and preliminary risk assessment. Sci. Total Environ. 387, 128–140.
Simpson, S.L., 2005. Exposure-effect model for calculating copper effect concentrations in sediments with varying copper binding properties: a synthesis. Environ. Sci. Technol. 39, 7089–7096.
Simpson, S.L., Angel, B.M., Jolley, D.F., 2004. Metal equilibration in laboratory-contaminated (spiked) sediments used for the development of whole-sediment toxicity tests. Chemosphere 54, 597–609. https://doi.org/10.1016/j.chemosphere.2003.08.007.
Simpson, S.L., Ward, D., Strom, D., Jolley, D.F., 2012. Oxidation of acid-volatile sulfide in surface sediments increases the release and toxicity of copper to the benthic amphipod *Melita plumulosa*. Chemosphere 88, 953–961. https://doi.org/10.1016/j.chemosphere.2012.03.026.
Thiel, J., Byrne, J.M., Kappler, A., Schink, B., Pester, M., 2019. Pyrite formation from FeS and H_2S is mediated through microbial redox activity. Proc. Natl. Acad. Sci. U.S.A. 116, 6897–6902. https://doi.org/10.1073/pnas.1814412116.
Thompson, A., Attwood, D., Gullikson, E., Howells, M., Kim, K.J., Kirz, J., Kortright, J., Lindau, I., Pianetta, P., Robinson, A., Scofield, J., Underwood, J., Williams, G., Winck, H., 2009. X-ray Data Booklet. Lawrence Berkeley National Laboratory, University of California, Berkeley, California.
Tiberg, C., Sjöstedt, C., Persson, I., Gustafsson, J.P., 2013. Phosphate effects on copper(II) and lead(II) sorption to ferrihydrite. Geochem. Cosmochim. Acta 120, 140–157.
Tostevin, R., Poulton, S.W., 2019. Oxic sediments. In: Gargaud, M., Irvine, W.M., RicardAmils, R., Cleaves, H.J., Pinti, D., Quintanilla, J.C., Viso, M. (Eds.), Encyclopedia of Astrobiology, Living Edition. Springer, Berlin, Germany, ISBN 978-3-642-27833-4.
U.S. Environmental Protection Agency, 1996. Method 6010B: Inductively Coupled Plasma-Atomic Emission Spectrometry.
U.S. Environmental Protection Agency, 2000. Methods for Measuring the Toxicity and Bioaccumulation of Sediment Associated Contaminants with Freshwater Invertebrates, second ed. USEPA Office of Research and Development, Duluth. EPA/600/R-99/064.
U.S. Environmental Protection Agency, 2002. Methods for Measuring the Acute Toxicity of Effluents and Receiving Waters to Freshwater and Marine Organisms, fifth ed. U.S.

Environmental Protection Agency, Office of Water, Washington, DC. EPA/821/R-02/012.
U.S. Environmental Protection Agency, 2005. Procedures for the Derivation of Equilibrium Partitioning Sediment Benchmarks (ESBs) for the Protection of Benthic Organisms: Metal Mixtures (Cadmium, Copper, Lead, Nickel, Silver, and Zinc). EPA-600-R-02–011, Washington, DC.
Vogt, H., Chattopadhyay, T., Stolz, H., 1983. Complete first-order Raman spectra of the pyrite structure compounds FeS_2, MnS_2 and SiP_2. J. Phys. Chem. Solid. 44, 869–873.
Weber, F.A., Voegelin, A., Kaegi, R., Kretzschmar, R., 2009. Contaminant mobilization by metallic copper and metal sulphide colloids in flooded soil. Nat. Geosci. 2, 267–271.
Yan, F., Schubert, S., Mengel, K., 1996. Soil pH increase due to biological decarboxylation of organic anions. Soil Biol. Biochem. 28, 617–624.
Yang, Y., Liu, W., Chen, M., 2013. A copper and iron K-edge XANES study on chalcopyrite leached by mesophiles and moderate thermophiles. Miner. Eng. 48, 31–35.
Yuan, C., Mosley, L.M., Fitzpatrick, R., Marschner, P., 2015. Amount of organic matter required to induce sulfate reduction in sulfuric material after re-flooding is affected by soil nitrate concentration. J. Environ. Manag. 151, 437–442.
Zhang, C., Yu, Z.G., Zeng, G.M., Jiang, M., Yang, Z.Z., Cui, F., Zhu, M., Shen, L., Hu, L., 2014. Effects of sediment geochemical properties on heavy metal bioavailability. Environ. Int. 73, 270–281. https://doi.org/10.1016/j.envint.2014.08.010.
Zimmerman, C.F., Keefe, C.W., Bashe, J., 1997. Method 440.0 Determination of Carbon and Nitrogen in Sediments and Particulates of Estuarine/Coastal Waters Using Elemental Analysis. U.S. Environmental Protection Agency, Washington, DC, USA. EPA/600/R-15/009.